Asian Journal of Chemistry; Vol. 24, No. 3 (2012), 1118-1124

ASIAN JOURNAL OF CHEMISTRY

www.asianjournalofchemistry.co.in

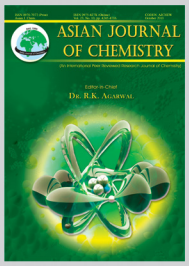

Structural Characterization of Mullite Formed from Heated Kaolin of Tamazert deposit (Algeria)

F. ZIBOUCHE[1,*], H. KERDJOUDJ[2] and TAHER ABADLIA MOHAMED[3]

[1]Laboratoire Matériaux Minéraux et Composites (LMMC), Faculté des Sciences de l'Ingénieur, Université de Boumerdès, 35000 Boumerdès, Algeria
[2]Laboratoire Hydrométallurgie et Chimie Inorganique Moléculaire, Université des Sciences et Techniques, Houari Boumédienne, Alger, Algeria
[3]Materials Engineering Deparment, Faculty of Engineering, University M'hamed Bougara, Boumerdes, Algeria

*Corresponding author: Fax: +213 24 9138 66; Tel: +213 24 819424; E-mail: zibouchefatima@yahoo.fr

(*Received*: 16 February 2011; *Accepted*: 7 November 2011) AJC-10607

A quantitative analysis of the mullite phase obtained after sintering of the kaolin has been performed by treatment of X ray diagrams. Kaolin is treated in the range of 950-1400 ºC. The oxide NiO is added as internal standard after cooling to sintered sample kaolin. Bragg Brentano diffractometer, scanning electron microscopy and differential thermal analysis were used. Analyses of selected directions profile of mullite were carried out by using the adjustment of program, available in the software Highscore of Pan Analytical. The mullite phase that formed from kaolin appears at 1000 ºC, observed by XRD and tallies with DTA. The primary mullite crystal showed a plate-like morphology. Two kinds of morphology corresponding to primary (elongated grains) and secondary (equiaxed grains) mullite were observed. A bimodal crystallite size distribution was detected through XRD microstructural analysis from 1300 ºC. The apparent sizes obtained of crystallites are determined for mullite with directions-dependent (anisotropy).

Key Words: Kaolin, Mullite, Quantitative analyses of phases, X-Ray methods.

INTRODUCTION

Kaolinitic clays are usually used to make fire-clays. The kaolin of Tamazert deposit is also used for the elaboration of "refractory bricks" which can replace those were defected in the furnaces of the whitewares factory of Mila town in the northeast of Algeria[1]. Kaolin has the advantage to be easily accessible and not expensive in natural open work seams[2]. It is a cheaper alternative ways of mullite synthesis using raw materials and a frequent subject of research[3-9], have been done about structural modifications that occur during the transformation of raw material to mullite and quantitative analysis. McGee and Wirkus[6] and Li and Thomson[7] have given data resulting from the application of the Scherer equation. Serrano *et al.*[8] and Sainz *et al.*[9], have shown microstructural analysis from a more developed X-ray diffraction profile line analysis.

The interpretation of wide line profile is more important in structural analysis. XRD line broadening is due to specimen and experimental factors. Experimental wide line profile is usually, described because of instrumental factors[10] and convolution specimen[11]. The effect "materials" are numerous, as inhomogeneous distribution in the composition of the material, the anisotropy, the size of the diffraction coherent areas, the local distortions of network, the impalement defaults *etc*. The XRD line profile is defined by its form parameter (Gaussian, Lorentzian, *etc*.), its FHWM (full width at half the maximum intensity), its integrated width β and Fourier coefficients. Within the former, the small size of crystal domains (crystallites) and the lattice strains of the specimen are the two main causes for line broadening, whereas wavelength distribution and geometric instrumental aberrations are the other factors that contribute to line broadening.

Size and strain parameters corresponding to the diffracting sample can be determined simultaneously by using several XRD line profile analysis methods. They are independent of the crystal nature. One of these methods is the well-known procedure of Warren and Averbach[12], which is based on the analysis of the Fourier coefficients. Another method, such as the Voigt function method[13], is based on a simplified procedure in which the size and strain parameters can be extracted from the precise XRD pattern of a single peak.

The methods of XRD quantitative analysis require accurate intensity measurements. The X-ray diffraction peaks area from diagrams (I, 2θ), gives information about quantitative phase which is present in sample materials. The phase which is on important content, shows peak area greater than others do minors phases. This area is called integrated area. We can make a quantitative analysis, with a calibration. (1 % mass is corresponding to 10 mg of phase for sample of 1 g)[14]. By far the methods in most general use involve addition of a known

amount of an internal standard and ratio in the standard peaks to that of the phases being determined. The method of standard additions requires a variety of diffraction patterns run on prepared samples in which varied amounts of a well-known standard, B, are added to the unknown mixture containing phase A, each mixture is analyzed. The internal standard method or modifications of it, is the most widely applied technique for quantitative XRD. The ratio of the two intensity equations we obtain:

$$\frac{I_{(h,k,l)_A}}{I'_{(h,k,l)_B}} = k\frac{X_A}{X_B}$$

where A is the phase to be determined, B is the standard phase and k is the calibration constant derived from a plot of $I_{(hkl)_A}/I_{(hkl)'_B}$ *versus* X_A/X_B. Direct application of this method requires careful preparation of standards to determine the calibration curves, but can produce quantitative determinations of identified phases that are substantially independent of other phases in the sample. Care must be taken when choosing standards to select materials with simple patterns (ideally an F-centred cubic structure) and well-defined peaks that do not overlap peaks in phases of interest. It is also very important that the crystallite size of the sample and standard being the same, ideally about 1 μm.

In the present work, the microstructural studies of the samples obtained by reaction sintering of Tamazert kaolin between 950 and 1400 ºC were performed mainly by XRD line profile analyses and by SEM studies. Quantitative analysis of diffraction data of mullite was followed. The aim of this paper is the study of the microstructural parameters deduced from line profile analysis and their compareson with microstructural features derived from SEM observations.

EXPERIMENTAL

The starting materials were commercial kaolin (Soalka, Algeria) with D (50 %): 84.464 μm, Ss = 14.466 m^2/g and high purity oxide NiO (from Merck). The kaolin was isocratic pressed at 200 MPa to form green compacts. Samples were cut into pellets 10 mm high and 7 mm in diameter and fired in air at a heating rate of 5 ºC/min up to different temperatures (950-1400 ºC) where they were soaked for 2 h and then cooled. The obtained forms were studied by XRD and SEM.

Methods of line profile analysis: Methods of XRD line profile analysis were used to obtain information about microstructural characteristics of the diffracting sample. The parameter most used to estimate the widening is the FHWM (full width at half the maximum intensity). Size and strain parameters corresponding to the diffracting sample can be determined simultaneously by using several XRD line profile analysis methods. Analyses of selected directions profile of mullite were carried out by using the adjustment of program, available in the software Highscore of Pan Analytical.

Voigt function[13]: This method is a simplified procedure permitting determination size and strain parameters from the precise XRD pattern of a single peak. The diffraction profile is assumed to be Voigtian (convolution of Cauchy and Gaussian profiles) because it has been proved[15] that the real diffraction profiles are well adjusted to the Voigt function. The Cauchy and Gaussian components of the measured profiles are related to the microstructural parameters (size and strain) of the diffracting sample. The formula used for the size parameter is:

$$D_v = \frac{\lambda}{\beta_{cf}\cos\theta}$$

$\langle D_v \rangle$ corresponds to the crystallite size, β_{cf} is the integral breadth of the Cauchy component of the real profile expressed in radian, λ is the wavelength used and θ the Bragg angle for the α_1 component. On the other hand, the strain parameter is given by:

$$e = \frac{\beta_{gf}}{4\tan\theta}$$

β_{gf} is the integral breadth of the Gaussian component of the real profile expressed in rad.

Warren-Averbach method[13]: This method is based on the analysis of the coefficients of the Fourier series that describe the XRD profiles and it is usually considered to be an accurate tool for the microstructural characterization of crystalline samples. This method requires at least two orders of the same reflection corresponding to the studied sample in order to separate the contributions to the peak broadening produced by domain size and strains. The XRD line profiles obtained for the two selected peaks (110) and (220) in this case of sample and standard in order to evaluate the crystallite size in the [110] direction; this has been possible because these reflections are intense and relatively isolated (no overlapping with other peaks).

Williamson and Hall method[11]: The reference element in the analysis of the profiles is the coherent area of diffraction (crystallite), given by the formula of Scherer:

$$\beta = \frac{K\lambda}{D\cos\theta}$$

D is the average size of the coherent measured areas following the vector of distribution for (hkl). K = 0.9-1.0: constant of Scherer. The effect of microdeformations (e: microdeformation averages fields of deformations) translates the existence of a non-uniform distortion of the crystalline network. To separate the effects of sizes of those of microdeformations, it is necessary to know the appropriate width for the lines of diffraction of at least a family of perpendicular plans (shots) in the same crystallographic direction (management). For that purpose, Williamson and Hall have used a semi quantitative method using both effects at the same time. They showed there is a relation between appropriate width β, ($\beta = K\lambda/D\cos\theta$), lines of diffraction corresponding to a crystallographic direction given and the rate of microdeformation e, ($\beta = 4e\tan\theta$), according to the same axis:

$$\beta = \frac{K\lambda}{D\cos\theta} + 4e\tan\theta$$

Quantitative analysis: Kaolin samples are heated to temperatures between 1000 and 1250 ºC. They are then cooled in the air after a landing of 5 min. After cooling, an internal standard is added to the samples[15,16]. The NiO has been chosen as internal standard[17], because it does not present superposition of peaks with other phases present in the range of chosen

measures, ($30^\circ < 2\theta > 43^\circ$). The mullite lines (110), (001) and (111) and the NiO line band (003) are selected.

A commercial mullite, called NOBALTEC. M 72 is used to study NiO-mullite mixtures. In the witness samples, a fixed amount of NiO, (m = 25 mg) is added at increasing rate of mullite. Curves of calibration necessary for the semi quantitative analysis are obtained. The determination of the quantity of mullite present in samples treated thermally was realized by adding 25 mg of NiO to 0.5 g of kaolin and crushed in a mortar agate. The ratio of the intensities is determined by a treatment of patterns. The curves of calibration representing the evolution of the ratios of the intensities of $\frac{I_{mullite}}{I_{mullite} + I_{NiO}}$ are drawn as function of mass ratios of $\frac{M_{mullite}}{M_{NiO}}$ for the three reflexions of the mullite.

X-Ray diffraction measurements: For XRD analyses a small quantity of fired material at different temperatures was ground with a tungsten carbide mortar and pestle to obtain finely powdered samples. The powders obtained were identified by XRD powder methods, indexed considering the mullite X-ray measurements using a conventional Philips PW1710 diffractometer operating at 40 Kv and 40 mA and interfaced to a DEL-PC running the X'Pert HighScore PC software package. Ni filtered CuK_α radiation was used.

X-Ray diffraction powder patterns over the range 5-60º (2θ) were performed for crystalline phase identification. The 110, 120, 210, 001, 220, 111 and 121 reflections of mullite were selected for line profile analysis performed in XRD patterns of powder samples. The experimental conditions for data collection were as follows: Step width of 0.020º (2θ) and measurement times of 2s was used in XRD patterns.

Standard profiles, needed for the evaluation of instrumental line broadening in selected X-ray patterns, were obtained from purified marketed mullite NOBALTEC. M72. The line profile analyses of selected reflections of mullite were performed by using the program FIT, available in the software package X'Pert Highscore. The experimental profiles were fitted to analytic functions (pseudo-Voigt and split-Pearson VII) after subtraction of an adjusted linear background and taking into account the effect of the CuK_{α_2} component on the experimental profile. The parameter used to estimate the goodness of the fit was R_{pf} (R: reliability, pf: profile fitting) defined as:

$$R_{pf} = \left[\frac{\Sigma (I_{obs} - I_{cal})^2}{I_{obs}^{é}} \right]^{0.5} \times 100$$

where, I_{obs} and I_{cal} are the observed and calculated intensity[18], respectively. The initial data used for the application of the Voigt function and the Warren-Averbach methods were obtained from the profiles fitted to analytical functions.

Microscopic observation: SEM has performed microscopic observations on samples fired between 1200 and 1400 ºC. The samples were cut into disks and finely polished using 6, 3 and 1 mm diamond suspension. Then were also thermal etches between 1200 and 1400 ºC for 0.5 h and chemical etches with a 10 % HF solution for 30 s. The SEM included a digitalized microscope (model HITACHI S-2500.

RESULTS AND DISCUSSION

Mullite phase transformation in kaolin: The X-rays diffraction spectra (Fig. 1) shows that the quantity of mullite formed just after the exothermic transformation of the metakaolin depends little on the speed of heat treatment. The first crystals of mullite obtained from the KF3 kaolin thus appear directly starting from the metakaolin or from the amorphous phase, whatever the speed of heat treatment and without passing through the spinal phase. Fig. 2 shows that the background noise between the 15-30 ºC stays until around 1000-1175 ºC. We will see thereafter that it increases in a significant way with the temperature. The intensities of the peaks allow comparing directly the quantities of mullite present after cooling. The samples treated with more than 1050 ºC show weak peaks of mullite phases. Until 1100 ºC there is no change, but from 1175 ºC, the intensity of the peaks of diffraction of mullite increases. The peaks of mullite intensify rise in the temperature progressively (Fig. 3). The unfolding of the lines (hk0) and the reflexions (hk0) of mullite start with 1350 ºC might imply the transformation of primary mullite towards an orthorhombic mullite (3:2 mullite).

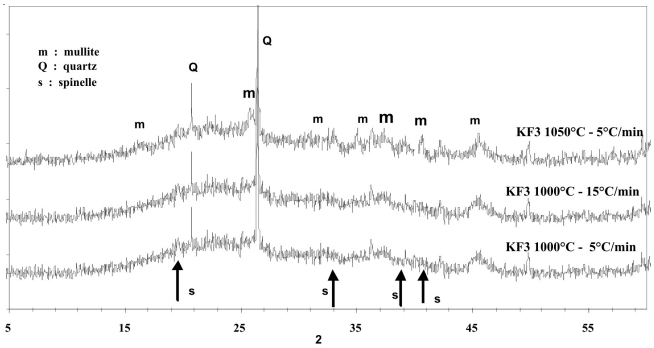

Fig. 1. Kaolin heated at 1000 ºC and an increase of temperature from 5-15 ºC/min

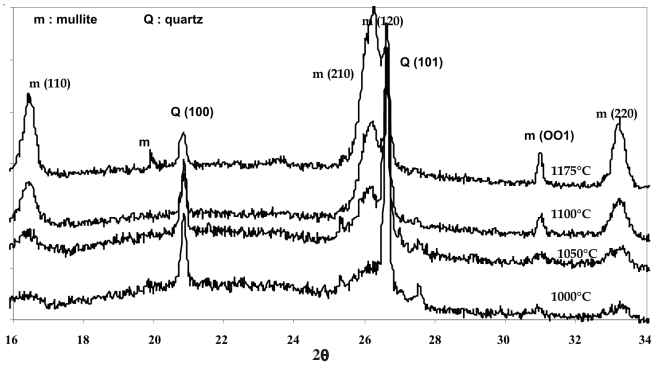

Fig. 2. Zoom between 15-35º 2θ of X ray diagrams from kaolin samples heated between 1000 and 1175 ºC

Fig. 2 presents X-rays patterns of samples treated at 1000-1175 ºC. The intensity of the background noise characteristic of the amorphous phase (centred to the 23º; 2θ) (Fig. 1), changes towards a weaker angle (21º; 2θ), (Fig. 2). However at this time, no cristobalite phase starts was not observed. The modifications are supposed to be connected to this exothermic reaction[19]. The surface of the peaks of diffraction in the diagrams (I, 2θ) may give information on the quantity of the

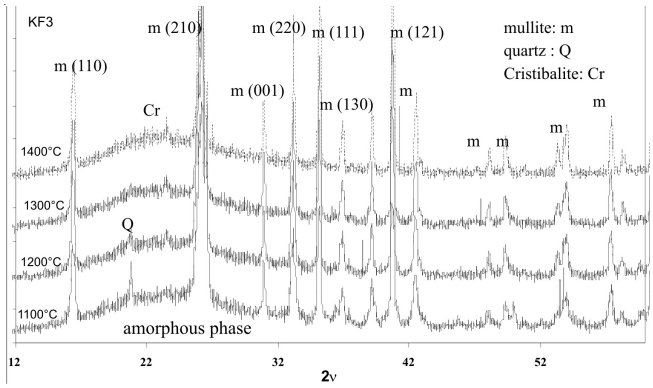

Fig. 3. X Ray patterns of kaolin samples heated between 1100-1400 ºC

phase present in the samples. When a phase is present in important proportion, the surface of its peaks is large: The clear surface means the area between the basic curve and continuous line. One can also say "integral intensity" to indicate this clear surface.

The duplication of lines (hk0) and reflections (hk0) of the mullite start at 1175 ºC (Figs. 2 and 3) which would involve the first transformation of the primary mullite (mullite 2:1) to a secondary mullite orthorhombic (mullite 3:2). It is noted that the mullite called "secondary" forms at *ca.* 1240 ºC, with an exothermic phenomenon.

Microstructure analysis of mullite phase in kaolin: The interpretation of the form of the profile of the widened lines is of primary importance in the analysis of the structural defects. Fig. 4 shows the X-ray diffraction pattern of the mullite standard, free of amorphous phase M72[16]. (JCPDS of Mullite: 01-079-1454), system orthorhombic, spatial group: Pbam55 and crystallographic parameters: a = 7.5811 Å, b = 7.6865 Å and c = 2.8892 Å.

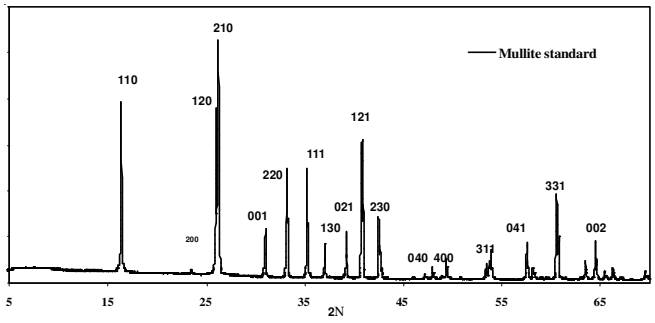

Fig. 4. X-Ray diffraction pattern of the mullite standard (NOBALTEC. M 72)

The patterns carried out on kaolin powders crushed and calcinated at 1100 and 1150 ºC during 5 min at 5 ºC/min and 20 ºC/min are shown in Fig. 5. They highlight the effects of widening of the lines of the kaolin treated at high temperature. The lines (110), (001), (220) and (111) of mullite are different according to the used heat treatment. For a given calcinations' temperature, the lines seem to be refined as the speed of treatment increases. In addition, they also seem to be refined when the calcination temperature increases for the same speed of heat treatment. This fact suggests the existence of the effect of size and/or microdistortions.

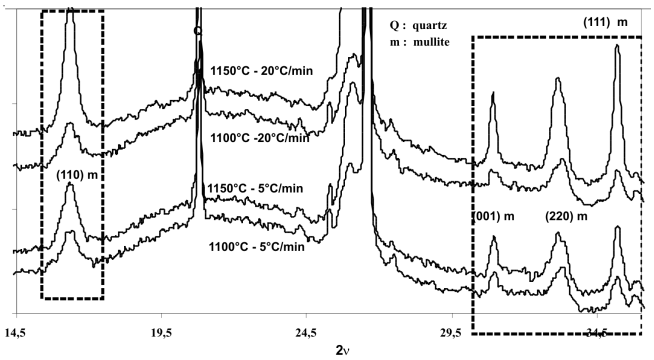

Fig. 5. Widening of diffraction lines (hk0) of Mullite of samples treated at 1100 and 1150 ºC with 5 ºC/min and 20 ºC/min rate

Fig. 6 shows the profile evolution of the 001, 220 and 111 reflexions of mullite, obtained from slow XRD patterns of samples heated at the range 1550-1650 ºC, used for the Voigt function methods. The XRD line profile analysis performed on the mullite samples obtained by sintering reaction of kaolin in the range 1100-1400 ºC is summarized in Table-1. On fired samples, the mullite crystallinity was estimated from line profile analysis of the selected reflections of mullite. Table-1 shows the parameters of the studied profile lines, it is possible to observe that the sample treated at 1400 ºC, presents the lowest values of the parameter 2w (width peak at half the maximum intensity) for all mullite reflections considered in the analysis. From Table-1 can also be deduced that the sample treated at 1400 ºC shows the better crystallinity.

Analysis of widening diffraction lines allows determination of defaults such as grain size or microdeformations[12]. The layout of the graph:

$$\beta\left(\frac{\cos\theta}{\lambda}\right)=\frac{1}{D}+e\left(\frac{2\sin\theta}{\lambda}\right)$$

Allows deducing the size from the particles L and the rate of microdistortion e.

TABLE-1
PARAMETERS OBTAINED FROM XRD MICROSTRUCTURAL ANALYSIS

Temperature fired sample	hkl								
	110			001			220		
	R_{pf} (%)	$2\theta_{obs}$ (º)	FWHM [2θ]	R_{pf} (%)	$2\theta_{obs}$ (º)	FWHM [2θ]	R_{pf} (%)	$2\theta_{obs}$ (º)	FWHM [2θ]
1100	0.29	16.3688	0.3936	9.64	30.9217	0.1181	1.25	33.1879	0.3149
1200	0.63	16.4003	0.1181	8.97	30.9020	0.1771	6.50	33.1868	0.1378
1300	6.30	16.4714	0.1574	1.23	30.8970	0.1968	11.72	33.2094	0.1378
1400	1.97	16.4797	0.0984	0.90	30.9262	0.1181	3.67	33.2313	0.1368
Mullite	0.12	16.4231	0.0836	0.90	30.9532	0.0612	6.97	33.1729	0.0816

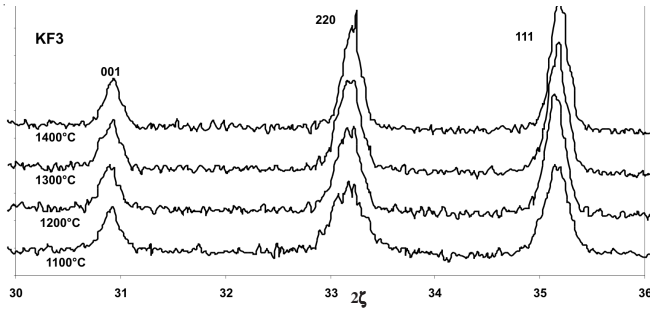

Fig. 6. Reflexions used in widening of diffraction lines analysis between 1100-1400 ºC

Figs. 7 and 8 present Williamson and Hall diagrams of mullite obtained from samples treated, respectively at 1100 and 1150 ºC, 5 and 20 ºC/min rate thermal treatment for (110), (220) and (001), (002) reflexions. The rate of microdistortions e of mullite presents in the samples of kaolin treated until 1150 ºC at 5 ºC/min is negligible in the directions (hk0) and (00l). On the other hand, the size of the particles is strongly anisotropic. The slope obtained is lower than 1.5 %. The widening of the lines of diffraction is due to size effect.

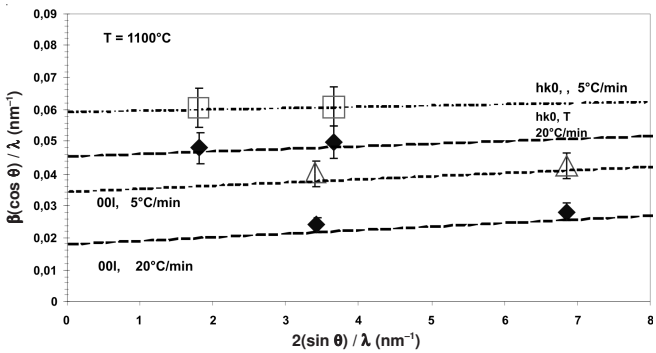

Fig. 7. Williamson and Hall diagram for the directions (hk0), (00l) of KF3 at 1100 ºC

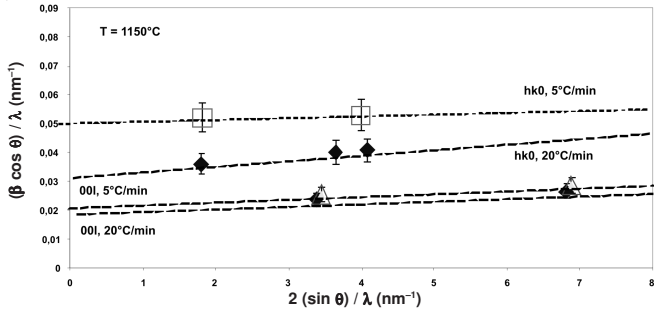

Fig. 8. Williamson and Hall diagram for the directions (hk0), (00l) of KF3 at 1150 ºC

Quantitative analysis: Using calibration, to make a quantitative analysis can be made. It concerns the calculation of the composition of the sample in percentage of mass (1 % of mass corresponds to 10 mg of phase for 1 g of sample). The calibration plots are obtained for the mixtures NiO-mullite. The graphs of calibration representing the evolution of the intensities ratios:

$$\frac{I_{mullite}}{I_{mullite} + I_{NiO}}$$

are drawn in function of masses ratio of: $\frac{M_{mullite}}{M_{NiO}}$ for the three selected reflexions of the mullite: (110), (001), (111) and (003) of NiO. Results are reported in Fig. 9. In fact, only the peak (111), nearer to the peak of the internal standard, is retained for the quantitative semi analysis. The percentage of mullite amounts in the range as 1050-1250 ºC are given in Table-2. The quantity of formed mullite is influenced by the speed of the heat treatment between 1050 and 1100 ºC. In this field, the mullite formation is clearly supported by a fast speed of the heat treatment. This difference is very marked for 1050 ºC (3, 25 and 6 %) and 1100 ºC (4, 25 and 10 %). This behaviour was already observed by previous workers[15,20]. The liquid phase appears only towards 1190 ºC. Mullite was developed without intervention of the liquid phase and may be result from the crystallization of new germs or the growth of those existing with 1000 ºC in the amorphous phase derived from the metakaolin.

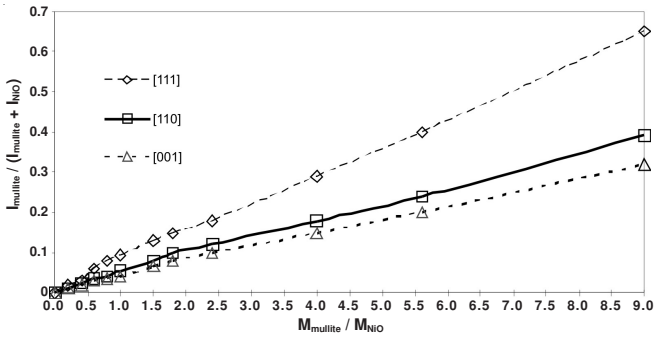

Fig. 9. Calibration lines used for the dosage of the mullite

TABLE-2
QUANTITY (%) OF MULLITE

Temperature (ºC)	1050	1100	1175	1250
Quantity at 5 ºC/min	3.25	4.25	13	15.5
Quantity at 15 °C/min	6	10	14	16

Around 1200 ºC, the liquid phase is present in large quantity and mullite develops by dissolution-crystallization. It was shown that the faster the heat treatment is, the more the metakaolin is disordered[20]. Knowing that consists of a juxtaposition of fields rich in aluminium and silicium. It seems that the influence of the speed of heat treatment on the crystallization of mullite in the phase derived from the kaolin of Tamazert is in agreement with this mechanism. Indeed, higher the speed of heating greater separation of the fields of disordered metakaolin. It would seem that the absence of phase spinal rich in aluminum is the result of the weak organization of the fields rich in aluminum.

Quantitative aspect of crystallites: The average size L according to directions (00l) and (hk0) of small mullite particles present in these samples are calculated from coordinates to the origin of diagrams of Figs. 7 and 8. The values obtained are reported on Table-3. The crystallites of mullite formed after 5 min of heat treatment at 1100 and 1150 ºC are highly anisotropic. They are lying along c axis whatever the heating rate. Between 1100 and 1150 ºC, the particle size increases with temperature. Meanwhile, the speed of heat treatment affects the size of crystallites.

TABLE-3
AVERAGE DIMENSIONS OF MULLITE PARTICULES

Temperature (ºC)	5 °C/min		20 °C/min	
	Direction [00l]	Direction [hk0]	Direction [00l]	Direction [hk0]
	L [nm]	L [nm]	L [nm]	L [nm]
1100	26 ± 3	16 ± 2	50 ± 3	22 ± 3
1150	48 ± 10	19 ± 3	50 ± 10	27 ± 3

The average volume of the mullite needles is simulated to that of parallelepiped. Knowing the average volume of the needles allow calculating the N_{aig} number of mullite needles per gram of KF3 kaolin starting from the results of Tables 2 and 3. The relation gives the number of needle per gram:

$$N_{aig} = \frac{M_{mullite}}{\rho_{mullite} \times V_{aig}}$$

The computed values of the average volume of the mullite crystals, the mullite mass per gram of powder and the number of needles per gram of powder per 10^{15}, are presented in the Table-4. Two tendencies exist according to the speed of heat treatment *e.g.*, when the speed of treatment is slow, (5 ºC/min), the number of needle increases with increasing of temperature; it passes from 3.82 10^{15} needles for a temperature of 1100 ºC, to 4.70 for a temperature of 1150 ºC. Consequently, the mullite particles would be always in phase of germination. On the other hand, when the speed of heat treatment is faster, the number of needles is not modified with the rise in temperature: it passes from 2.50×10^{15}, to 2.39×10^{15} for, respectively at 1100 and 1150 ºC.

TABLE-4
AVERAGE VOLUME, MASS/g AND A NUMBER OF MULLITE NEEDLES FOR THE VARIOUS CONDITIONS OF TREATMENT OF THE KAOLIN

Speed (°C/min)	Temp. (°C)	Mass of mullite/g of powder	Volume of crystals (nm^3)	Number of needles/g × 10^{15}
5	1100	0.04	$26 \times (16^2/2)$	3.82
	1175	0.13	$48 \times (19^2/2)$	4.70
20	1100	0.99	$50 \times (22^2/2)$	2.50
	1175	0.14	$50 \times (27^2/2)$	2.39

Morphology of the mullite particles: Fig. 10 shows that the formed mullite crystals after 2 h sintering with 1250 ºC, are generally in a great lengthening, in a distribution of narrow sizes and are aggregate. These results indicate that the primary mullite crystals are formed only starting from kaolinite (Fig. 10). After sintering at 1400 ºC/2 h, there is existence of large mullite crystals with a higher lengthening corresponding to the primary mullite developed in an amorphous matrix and smaller secondary mullite crystals (500 μn), proves that the morphology of grain seemed to be a mixture of secondary mullite crystals.

Conclusion

The studies suggest that the mullite particles are in phase of enlargement and thus, that a treatment having a fast speed favourites the enlargement of crystals. The analysis of profiles by X-rays diffraction, it is possible to observe, between 1300 and 1450 ºC, the simultaneous presence of two morphologies

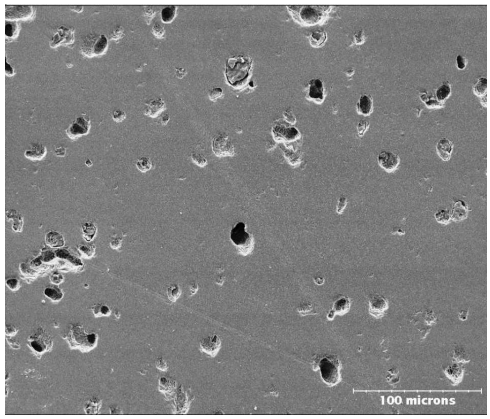

(a)

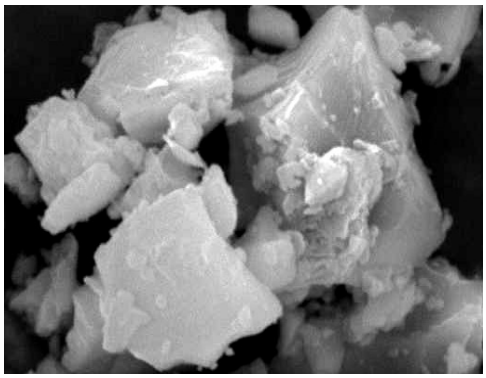

(b)

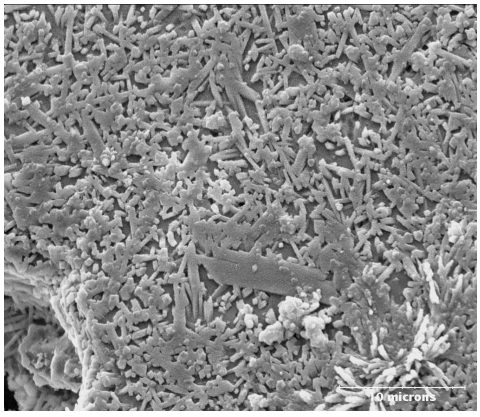

(c)

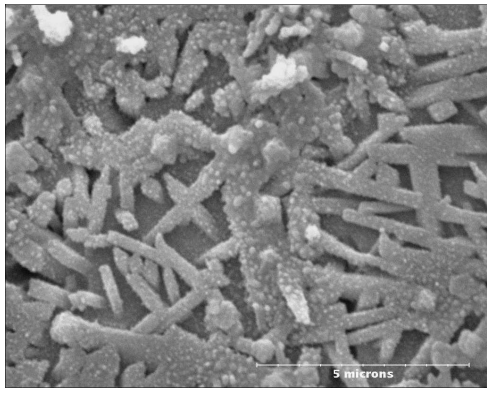

(d)

Fig. 10. (a) Mullite M72, (b) KF3 (1400 °C) without chemical attack, (c) KF3 1400 °C, after chemical attack, resolution 3000 and (d) with resolution 10000

of mullite and the evolution of the size of crystallite in the morphology of the mullite. The microstructural studies established that the crystals corresponding in the nucleation of secondary mullite and in the growth of primary mullite at 1300 ºC. The XRD also proved in the temperature between 1300 and 1400 ºC, the maximal sizes of crystallite are moved in bigger values, reflection the growth of crystallite. At the temperatures of 1400 ºC, the SEM proved that the primary and secondary mullite develops simultaneously. This evolution is typical for the mullite developed at high temperature in presence of a liquid permanent phase.

REFERENCES

1. M. Taib, The Mineral Industry of Algeria, 2009 Minerals Yearbook, U.S. Geological Survey (2011)..
2. H.H. Murray, *Appl. Clay Sci*., **17**, 207 (2000).
3. H. Schneider, K. Okada and J.A. Pask, Mullite and Mullite Ceramics, John Wiley & Sons, Chichester, UK, pp. 1-251 (1994).
4. J.L. Holm, *Phys. Chem. Chem. Phys*., **3**, 1362 (2001).
5. O. Castelein, B. Soulestin, J.P. Bonnet and P. Blanchart, *Ceramics Int*., **27**, 517 (2001).
6. T.D. McGee and C.D. Wirkus, *Bull. Am. Ceram. Soc*., **51**, 577 (1972).
7. D.X. Li and W.J. Thomson, *J. Am. Ceram. Soc*., **73**, 964 (1990).
8. F.J. Serrano, J. Bastida, J.M. Amigo and A. Sanz, *Crystallogr. Res. Technol*., **31**, 1085 (1996).
9. M.A. Sainz, F.J. Serrano, J.M. Amigo, J. Bastida and A. Caballero, *J. Eur. Ceramic Soc*., **20**, 403 (2000).
10. G. Berti, U. Bartoli, M.D. Acunto and F.D. Marco, *Mater. Sci. Forum Vols*, **443-444**, 27 (2004).
11. G.K. Williamson and W.H. Hall, *Acta Metall.*, **1**, 22 (1953).
12. B.E. Warren and B.C. Averbach, *J. Appl. Phys*., **21**, 595 (1950).
13. R. Delhez, T.H. Keijser and E.J. Mittemeijer, *Fresenius' J. Anal. Chem.*, **312**, 1 (1982).
14. R. Guinebretiere, Diffraction des Rayons X sur Echantillons Polycristallins, Edition Lavoisier (2002).
15. G.W. Brindley and G. Brown, *Mineral. Soc. Monogr.*, **5**, 323 (1980).
16. W. Chao, P. Chunde, W. Daqing, S. Aixia, N. Jihong and L. Shuhua. *Powder Diffraction*, **11**, 235 (1996).
17. A.F. Gualtieri, E. Mazzucato, P. Venturelli, A. Viani, P. Zannini and L. Petras, *J. Am. Ceram. Soc*., **82**, 2566 (1999).
18. G. Will, W. Parrish and T.C. Huang, *J. Appl. Crystallogr*., **16**, 611 (1983).
19. Y.-F. Chen, M.-C. Wang and M.-H. Hon, *J. Eur. Ceram. Soc*., **24**, 2389 (2004).
20. G. Brown, K.J.D. Mackenzie, M.E. Bowden and R.H. Meinhold, *J. Am. Ceram. Soc*., **68**, **6**, 298 (1985).